

# TrustyAI Explainability Toolkit

Rob Geada*	Tommaso Teofili *
Red Hat	Red Hat, Roma Tre University
rgeada@redhat.com	tteofili@redhat.com
Rui Vieira*	Rebecca Whitworth
Red Hat	Red Hat
rui@redhat.com	rsimmond@redhat.com
Daniele Zonca	
Red Hat	
dzonca@redhat.com	

## Abstract

Artificial intelligence (AI) is becoming increasingly more popular and can be found in workplaces and homes around the world. However, how do we ensure trust in these systems? Regulation changes such as the GDPR mean that users have a right to understand how their data has been processed as well as saved. Therefore if, for example, you are denied a loan you have the right to ask why. This can be hard if the method for working this out uses “black box” machine learning techniques such as neural networks. TrustyAI is a new initiative which looks into explainable artificial intelligence (XAI) solutions to address trustworthiness in ML as well as decision services landscapes.

In this paper we will look at how TrustyAI can support trust in decision services and predictive models. We investigate techniques such as LIME, SHAP and counterfactuals, benchmarking both LIME and counterfactual techniques against existing implementations. We also look into an extended version of SHAP, which supports background data selection to be evaluated based on quantitative data and allows for error bounds.

## 1 Introduction

Automation of *decisions* is crucial to deal with complex business processes that can responsively react to changes in business conditions and scenarios. The orchestration and automation of *decision services* [ZSEv12, HDVS20] is one of the key aspects in handling such business processes.

---

\*Equal Contribution

Decision services can work on fine-grained inputs, like assessing the risk of a single transaction, or on rather complex inputs (often hierarchical), commonly involving sub decisions to be taken and composed into a final decision. Decision services can leverage different kinds of *predictive models* underneath, from rule-based systems to decision trees [ESB19] or machine-learning based approaches [Ath17].

In this context, one important aspect is the trustworthiness of such decision services, especially when automated decisions might impact human lives. Decision services might not, in principle, be opaque as AI systems like the ones based on neural networks, but they still can be very hard to interpret and understand in practice, *e.g.* due to long lists of rules, complex / deep decision trees and so on. Besides, a decision service can integrate other AI-based systems (*i.e.* SVMs, neural networks) to produce the decision, making the whole process much less transparent.

For this reason, it is important to be able to *explain* decision services. Techniques from Explainable Artificial Intelligence (XAI) [Gun17, ADRDS<sup>+</sup>20] can therefore be adapted to address concerns about trustworthiness in decision services.

In this paper, we present the *TrustyAI Explainability Toolkit*<sup>1</sup>, an open source XAI library leveraging different explainability techniques for explaining decision services (*e.g.* based on business rules or open standards like DMN<sup>23</sup>) as well as AI-based systems in a black-box fashion. *TrustyAI*<sup>4</sup> is an initiative part of Kogito ecosystem<sup>5</sup> that aims to offer value-added services to a Business Automation solution.

In particular, the *TrustyAI Explainability Toolkit* leverages the following explainability techniques for black-box AI systems: LIME[RSG16], SHAP[LL17] and counterfactual explanation[WMR17].

We make the following contributions:

- To the best of our knowledge, the first comprehensive set of tools for XAI that works well in the decision service domain
- An extended approach for generating Local Interpretable Model-agnostic Explanations [RSG16], especially built for decision services
- A counterfactual explanation generation approach based on constraint problem solver

---

<sup>1</sup>TrustyAI Explainability Toolkit code: <https://github.com/kiegroup/kogito-apps/tree/master/explainability/explainability-core>, last accessed 29/03/2021.

<sup>2</sup>Decision Model and Notation, <https://www.omg.org/spec/DMN/About-DMN/>, last accessed 29/03/2021.

<sup>3</sup>Drools DMN implementation, <https://drools.org/learn/dmn.html>, last accessed 29/03/2021.

<sup>4</sup>TrustyAI page, <https://kogito.kie.org/trustyai/>, last accessed 29/03/2021.

<sup>5</sup>Kogito website, <https://kogito.kie.org/>, last accessed 29/03/2021.

- An extended version of SHAP [LL17] which enables background data identification and includes error bounds while generating confidence scores

## 2 Related work

There’s a plethora of existing toolkits in the XAI ecosystem. Known examples that address explainability for black box models are: Alibi [KVLVC19], an open source Python library aimed at machine learning model inspection and interpretation, Py-CIU [AKF20], a library for explaining ML predictions using contextual importance and utility , InterpretML [NJKC19], a framework providing interpretable models as well as post-hoc explanation methods (based on original papers implementations) DALEX [Bie18], an explainability toolkit written in R. Other interesting tools in the XAI ecosystem are the What-if tool [WPB<sup>+</sup>19] and LIT [TWB<sup>+</sup>20], an interactive model-understanding tool, with a focus on NLP models. To the best of our knowledge, none of the above mentioned tools has been designed with the decision service scenario in mind.

Counterfactual explanations were formally proposed originally by Wachter et al. [WMR17] in 2017 as an explainability device using a numerical optimization approach. Other approaches, such as gradient-free numerical solutions are proposed by Grath [GCV<sup>+</sup>18] and Thibault [LLM<sup>+</sup>18a] (2018). Research on additional desirable properties of counterfactuals, such as sparsity is performed by Miller et al. [Mil19], and for actionability by Karimi et al. [KBBV20] and Lash et al. [LLS<sup>+</sup>17]. Combinatorial optimization problems have a long research history, but in this paper we use techniques mainly developed by Glover [Glo89], such as *Tabu* search. The alternative implementation used for a baseline comparison was Alibi’s <sup>6</sup> counterfactual explanation, which is itself based on [WMR17] implemented using a Tensorflow [ABC<sup>+</sup>16] backend.

## 3 Robust LIME explanations

### 3.1 Background

Local Interpretable Model-agnostic Explanations (LIME) [RSG16] is one of the most widely used approaches for explaining a prediction  $p = (x, y)$  (an input-output pair) generated by a black box model  $f : \mathbb{R}^d \rightarrow \mathbb{R}$ . Such explanations come in the form of a weight  $w_i$  attached to each feature  $x_i$  in the prediction input  $x$ .

LIME generates a local explanation  $\xi(x)$  according to the following model:

$$\xi(x) = \operatorname{argmin}_{g \in G} L(f, g, \pi_x) + \Omega(g)$$

---

<sup>6</sup>Alibi, <https://github.com/SeldonIO/alibi>, last accessed 31/03/2021.

where  $\pi_x$  is a proximity function,  $G$  the family of interpretable models,  $\Omega(g)$  is a measure of complexity of an explanation  $g \in G$  and  $L(f, g, \pi_x)$  is a measure of how unfaithful  $g$  is in approximating  $f$  in the locality defined by  $\pi_x$ . In the original paper,  $G$  is the class of linear models,  $\pi_x$  is an exponential kernel on a distance function  $D$  (e.g. cosine distance). LIME converts samples  $x_i$  from the original domain into interpretable samples as binary vectors  $x'_i \in \{0, 1\}$ . An encoded dataset  $E$  is built by taking non-zero elements of  $x'_i$ , recovering the original representation  $z \in \mathbb{R}^d$  and then computing  $f(z)$ . A weighted linear model  $g$  (with weights provided via  $\pi_x$ ) is then trained upon the generated sparse dataset  $E$  and the model weights  $w$  are used as feature weights for the final explanation  $\xi(x)$ .

We extend the original LIME approach [RSG16] to make it robust in scenarios where either training data is not used to generate the original model or the training data used to fit the model is not available anymore. Similar to other works like [VG19], [LBS<sup>+</sup>19], [VBC20a], [Wen21], we adapt the original LIME approach to a specific scenario (the decision service domain) where the vanilla solution has proved to be not effective, or even not usable. We build on existing work trying to understand [ZSS<sup>+</sup>19] and fix LIME limitations: such works focus on improving the way LIME produces explanations, for example, by moving beyond linear approximation of local predictions to non-linear ones (via quadratic approximations) [BHTL20], or by incorporating intrinsic dependency information in the sampling strategy adopted by LIME [SDF20].

### 3.2 Robustness

As discussed in [VBC<sup>+</sup>20b], [LBS<sup>+</sup>19], [ZSS<sup>+</sup>19] LIME suffers from stability issues. Several different runs of LIME on the same  $x$  might generate different explanations  $\xi(x)$ . This undermines the faithfulness of the generated explanations and poses concerns about its usage in real-life scenarios.

As shown in [VŠ21] and [SSrHF19] the accuracy of explanations generated by LIME depends significantly on the sampling strategy.

Another aspect relates to the availability of training data. LIME uses the training data to define each feature’s perturbation space, when dealing with tabular data. This dependency makes it hard to generate accurate explanations when either the training data is not (fully) available or when the model does not use training data at all (*e.g.* rule-based systems, decision tables, etc.). This aspect is particularly important for decision services that often involve decision tables combined with machine learning-based systems.

### 3.3 Our method

We propose an extension of the LIME method to make it work when either the training set originally used to train a model is not available or the

model to explain does not use any training data (e.g. rule-based models). In addition, we adopt a few optimizations to address stability issues and situations where the sampled data is likely not to produce an accurate linear model.

### 3.3.1 Training data

The original LIME work leverages the existing data distribution  $F$ , used to train the model, to:

- generate appropriate values to perturb numerical features
- generate *buckets* for sparse encoding (a value  $v_{s_i}$  from a generated sample  $s$  is encoded as 1 if it falls within the same feature histogram bucket as the value  $v_{x_i}$  from the same feature  $x_i$  in the original input  $x$ )

We assume  $F$  is not available, as it is often the case in the decision service scenario.

For the generation of feature values to perturb numerical features, given the original value  $v_{x_i}$  from  $x_i$  we sample from a Gaussian distribution with mean  $\mu = v_{x_i}$  and standard deviation  $\sigma = 0.01 * v_{x_i}$ .

For the encoding part, given perturbed samples  $s \in S$  and the original input  $x_i$  we first perform max-min scaling of  $x_i \cup S$ , obtaining a new set  $S^\wedge$ . Given a Gaussian kernel  $\phi$  (with  $\mu = x_i^\wedge$  and  $\sigma = 1$ ) we set the threshold  $\theta = \phi(x_i^\wedge)$ . The encoded dataset  $E$  for  $S$  is

$$E = \{\text{sign}(|\phi(s^\wedge) - \theta|), \forall s^\wedge \in (S^\wedge \setminus x_i)\} \quad (1)$$

### 3.3.2 Adaptive dataset variance

The sampling strategy in LIME draws samples that should be as close as possible to the original input  $x$ . It is possible that the generated samples, when exposed to the model  $f$ , might all be predicted to have the same class. This can happen if all (or most of) the samples are very close to  $x$  or the  $f$  is biased with respect to  $x$ .

Given a set of samples with their predictions  $S = \{(s_i, f(s_i))\}$  we calculate the class balance  $\beta_S$  as the fraction of samples predicted as *true*.

We define the linear separability check as  $\nu = \beta_S > 0.1$

Each time a sampling dataset  $S$  is generated, we enforce a minimum no. of features  $\omega$  to be perturbed for each  $s \in S$  and the sampling dataset size  $z$ .

When  $\nu = \text{false}$  we generate a new sample  $S'$ , enforcing a bigger variance in the perturbation. We do so by

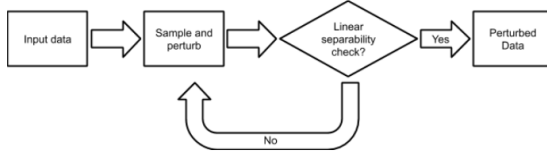


Figure 1: Adaptive dataset variance loop

- imposing a higher number of features  $\omega' = \omega + 1$  to be perturbed for each  $s \in S'$  (until  $\omega = |x| - 1$ )
- creating a bigger dataset with  $z' = 2 \cdot z$  so that  $|S'| = z'$

The adaptive dataset variance procedure can be summarized in figure 1.

### 3.3.3 Sparse dataset balance penalty

The quality of the generated sparse dataset  $E$ , used to train the interpretable model, is crucial for the effectiveness of the explanation. We observe that, due to either a suboptimal choice of samples or suboptimal sparse encoding, the sparse dataset  $E$  can be hardly separable with a linear decision boundary.

Let's consider  $E$  composed by sparse input values  $s_i$  paired with sparse output values  $o_i$ . We decide to penalize those features that, when taken independently, are balanced (input-wise) with respect to the two possible output classes ( $o_i \in \{0, 1\}$ ). We make the penalty worse when the number of features is low. The extreme case is the one where there is only one feature and  $E = \{(s_i, o_i)\}$  is the following:  $\{(0, 0), (0, 1), (1, 0), (1, 1)\}$ , which is clearly not separable.

For each feature  $x_k$  we calculate the class balance (in the interpretable space) for both possible outputs  $o \in \{0, 1\}$  so that

$$b_{o,k} = \frac{1}{|E|} \sum_{\{s_{i,k} | f(s_i)=o\}} s_{i,k} \quad (2)$$

We calculate the distance from the perfect balance, penalizing more as the distance becomes smaller; the biggest penalty will be given with  $b_{o,k} = 0.5$ .

$$d_{o,k} = |0.5 - b_{o,k}| \quad (3)$$

Finally, we set the penalty for a feature  $x_k$  to increase together with  $d_{o,k}$  and the number of features  $|x|$ ; the non-linearity introduced by  $\tanh$  serves as a smoothing function.

$$\eta_k = \tanh\left(\tau + d_{0,k} + d_{1,k} + \frac{|x|}{\rho}\right) \quad (4)$$

The resulting weight for each feature  $x_k$  is  $w'_k = w_k \cdot \eta_k$   
 In our experiments we set  $\tau = 0.01$  and  $\rho = 10$ .

### 3.3.4 Proximity filtering

We take suggestion from [LRL<sup>+</sup>18] to directly generate samples close to the original prediction, instead of the sample and weighting approach from the original LIME paper. We adopt  $\pi_x$  to determine which samples should be taken and which ones should be discarded and not used for the linear model fitting. More formally, given the set of generated samples  $S$ , the filtered dataset  $\hat{S}$  is

$$\hat{S} = \{s \mid \pi_x(s) \geq \kappa, \forall s \in S\} \quad (5)$$

In our experiments, we set  $\kappa = 0.8$ .

## 3.4 Experiments

### 3.4.1 Predictive models and data

For the evaluation of the effectiveness of TrustyAI LIME approach (*LIME-TrustyAI*) we use the model and data described in section 5.3.1.

### 3.4.2 Metrics and methodology

To evaluate the effectiveness of a LIME explanation, we leverage the *impact-score* described in [LSB<sup>+</sup>19]. This quantitative evaluation aims at capturing whether our approach actually produces explanations that better capture the important features. We evaluate the *impact-score* on the explanations generated by LIME for all the inputs in the training set. We conduct experiments with the no. of important factors  $c$  (no. of features to be dropped) for the impact-score calculation set to 1 and 2. For each experimental setting, we run the experiments 10 times and report minimum and maximum obtained *impact-score*.

### 3.4.3 Baselines

We benchmark our approach against the official implementation from the LIME paper <sup>7</sup>, both with discretized (*LIME-discr*) and continuous features (*LIME-cont*). Feature discretization for numerical features enables computation of feature mean / standard deviation and then discretization into quartiles.

---

<sup>7</sup>LIME reference implementation: <https://github.com/marcotcr/lime>

### 3.4.4 Results

In table 1 we report the *impact-score* of obtained on the model described in section 5.3.1 with TrustyAI and the mentioned baselines.

LIME implementation	$c$	Impact-score
LIME-cont	1	0.01-0.02
LIME-discr	1	0.07-0.1
LIME-TrustyAI	1	0.51-0.53
LIME-cont	2	0.06-0.1
LIME-discr	2	0.12-0.17
LIME-TrustyAI	2	0.40-0.43

Table 1: Impact-score evaluation of baseline LIME implementations (continuous and discrete features settings) vs TrustyAI LIME implementation, with different critical factors size  $c = \{1, 2\}$

We observe a significant improvement in *impact-score* when using TrustyAI. It is important to note that, for the sake of the experiment, we used the training data to generate explanations with *LIME-cont* and *LIME-dist*, whereas we did not use any such data with the *LIME-TrustyAI*.

Additionally, we note that the *impact-score* increases with  $c$  on *LIME-cont* and *LIME-dist*. The same doesn't apply to *LIME-TrustyAI*, in fact the *impact-score* decreases when  $c = 2$  with respect to  $c = 1$ . This indicates that *LIME-TrustyAI* is better at finding the top *single* influential feature for a given prediction; it is slightly less accurate at finding the top 2 influential features, while still outperforming the official LIME implementation by 0.23.

## 4 SHAP

We have not yet performed full benchmarks of our SHAP implementation (*SHAP-TrustyAI*), as we are still working to ensure that it is fully compatible with the TrustyAI toolkit. As such, this section will instead focus on how we intend to extend SHAP and some of the issues in existing implementations that we hope to address, specifically that of *background data choice* and *attribution confidence*.

### 4.1 Background

SHAP [LL17], presented by Scott Lundberg and Su-In Lee in 2017, seeks to unify a number of common explanation methods, notably LIME [RSG16] and DeepLIFT [SGK17], under a common umbrella of *additive feature attributions*. These are explanation methods that explain how an input  $x =$



$[x_1, x_2, \dots, x_M]$  affects the output of some model  $f$  by transforming  $x \in \mathcal{R}^M$  into *simplified inputs*  $z' \in 0, 1^M$ , such that  $z'_i$  indicates the inclusion or exclusion of feature  $i$ . These simplified inputs are then passed to an explanatory model  $g$  that takes the following form:

$$x = h_x(z') \quad (6)$$

$$g(z') = \phi_0 + \sum_{i=1}^M \phi_i z'_i \quad (7)$$

$$\text{such that } g(z') \approx f(h_x(z')) \quad (8)$$

In such a form, each value  $\phi_i$  marks the contribution that feature  $i$  had on the output model (called the *attribution*), and  $\phi_0$  marks the *null output* of the model; the model output when every feature is excluded. Therefore, this presents an easily interpretable explanation of the importance of each feature and a framework to permute the various input features to establish their collection contributions.

However, where the various methods unified under this form vary are in their methodology for choosing those  $\phi$  values. Lundberg and Lee therefore determine three desirable attributes of such an additive feature attribution: *local accuracy*, *missingness*, and *consistency*. Briefly, local accuracy enforces that  $g(z') \approx f(h_x(z'))$ , missingness enforces  $z'_i = 0 \implies \phi_i = 0$ , and consistency that  $\phi_i(f', x) \geq \phi_i(f, x)$  if  $f'(z') - f'(z'/i) \geq f(z') - f(z'/i)$ , where  $z'/i$  marks the exclusion of feature  $i$  from  $z'$ . Each of the attributes place constraints on the possible choices of  $\phi$  such as to maintain the logical integrity of the explanations. Lundberg and Lee argue that there exists only one such solution that maintains all three properties, one such that the values of  $\phi$  are chosen to be Shapley values [Sha53], and define a loss function  $\mathcal{L}$  whose minima returns these values:

$$\pi_{x'}(z') = \frac{(M-1)}{(M \text{ choose } |z'|)|z'|(M-|z'|)} \quad (9)$$

$$\mathcal{L}(f, g, \pi_{x'}) = \sum_{z' \in Z} |f(h_x(z')) - g(z')|^2 \pi_{x'}(z') \quad (10)$$

where  $M$  is the number of features in  $x$  and  $|z'|$  is the number of included features in  $z'$ . This loss can be solved via a weighted linear regression, through sampling a variety of permutations of  $z'$  and observing how they change the output of the model.

To allow for the exclusion of arbitrary features without modification or re-training of the model, Lundberg and Lee formulate an approximation of exclusion through the use of *background data*  $B$ , a collection of  $N$  representative data points that should ideally represent the “average” inputs to the

model. With this, they define the output of a model with missing features as:

$$\bar{X}_{n,i} = \begin{cases} z'_i = 0, & B_{n,i} \\ z'_i = 1, & x_i \end{cases} \quad (11)$$

$$f(x | z', B) = E(f(\bar{X}_n) | n \in 0, \dots, N) \quad (12)$$

This combines the original data point  $x$  with the background data points, such that the excluded features in  $x$  are replaced with the values taken by those features in the background data, while included features are left untouched. One of these synthetic data points are generated for each of the  $N$  data points in  $B$ , and the expectation of the model output over all such synthetic data points is used to approximate the effect of excluding these features. The rationale is that this emulates replacing a particular feature with the “average” value, thus nullifying any difference it creates.

## 4.2 Background Data Choice

The disadvantage of exclusion via background data is that it renders all feature attributions as comparisons to the background data, not against “true” exclusion. The best way to visualize this problem is by looking at a very simple model, one whose feature attributions are readily apparent:

$$f(x) = \sum_i^M x_i \quad (13)$$

For any input vector,  $\phi_i$  should equal  $x_i$  and the null output  $\phi_0$  should equal zero; each feature contributes its exact value to the output and omitting every feature would result in an output of zero. For example, given  $x = [1, 2, 3, 4]$ ,  $\phi_0 = 0$  and  $\phi = [1, 2, 3, 4]$ . We can also look at this model and pick background data that represents true feature exclusion:  $[[0, 0, 0, 0]]$ . Under this setting, SHAP returns the exact attributions that we would expect:

Null Output	$\phi_1$	$\phi_2$	$\phi_3$	$\phi_4$
0.0	1.0	2.0	3.0	4.0

Table 2: Feature attributions for our simple model (equation 13) for  $x = [1, 2, 3, 4]$  and  $B = [[0, 0, 0, 0]]$ .

However, our choice of background data in this example is problematic; we knew exactly how exclusion affects our model and could pick  $B =$

[[0, 0, 0, 0]] because we knew that excluding a particular feature is equivalent to setting it to 0. For the majority of real-world models, especially for black-box ML models, such a targeted and informed choice of background data will not be possible. In such an instance, our choice of background data (often an arbitrary sample of the training data) will be less informed. We can simulate how this would affect the interpretability of our feature attributions by choosing a less informed background dataset for our example model, this time drawing 100 background data points from a uniform distribution across  $[0, 10]$ :

Null Output	$\phi_1$	$\phi_2$	$\phi_3$	$\phi_4$
20.36	-3.85	-3.23	-2.34	-0.93

Table 3: Feature attributions for our simple model (equation 13) for  $x = [1, 2, 3, 4]$  and  $B$  drawn from  $\mathcal{U}(0, 10)$ .

While these feature attributions are all still accurate, in that  $20.36 - 3.85 - 3.23 - 2.34 - 0.93 = 10 = 1 + 2 + 3 + 4$ , what they represent becomes less useful and less intuitive. They now indicate the contribution each feature makes against the expectation of the model over the background data, that the inclusion of feature 1 from  $x$  causes an average change of -3.85 compared to the values of feature 1 in  $B$ . This is an excellent illustration of the issue that can stem from the choice of background data: SHAP feature attributions represent an arbitrary comparison if  $B$  is chosen arbitrarily.

Determining a method for identifying background datasets that provide intuitive feature attributions is an active area of research in the TrustyAI initiative. One potential option is to adapt the extensions to LIME as described in section 3.3.1, where the dependence on the original training data is circumvented. Another option is to ask the user to specify an intuitive ‘null output’ of the model based on their intuition and then attempt to identify a background dataset that produces as similar ‘null output’ as possible.

### 4.3 Attribution Confidence

The feature attributions provided by SHAP are generated by solving a weighted linear regression. In a real-world use-case, the regression variables will be comprised of a variety of samples of synthetic data passed through an imperfect model; there will be noise in the regression variables and thus implicit error in the regression model. The existing implementation of SHAP [LL21] does not present confidence intervals or error bars in the found feature attributions, a problem which can be uncovered by comparing the predicted attributions with observed attributions. We will use the minimal credit card approval example described in section 5.3.1. Using the first 100 training data points of the model as  $B$  and attempting to explain

$x = [\text{Age: } 27.250, \text{Debt: } 0.625, \text{YearsEmployed: } 0.455, \text{Income: } 0.000]$ , we get the following feature attributions:

Null Output	Age	Debt	YearsEmployed	Income
0.837	-0.009	0.056	0.061	0.025

Table 4: Feature attributions for our credit card approval model (section 5.3.1) for  $x = [27.250, 0.625, 0.455, 0.000]$  and  $B$  equal to the first 100 training data points.

Our model predicts that this particular applicant has a 97.0% rejection probability, with *Debt* and *YearsEmployed* contributing greatest to the 14 percentage point increase from the null output.<sup>8</sup> We can then attempt to validate these attributions by dropping each feature and looking at the expectation of the synthetic input  $\bar{X}$ :

Dropped Feature	Age	Debt	YearsEmployed	Income
Predicted Value $f(x) - \phi_i$	0.979	0.914	0.909	0.945
Observed Value $E(f(\bar{X}))$	0.946	0.894	0.899	.898

Table 5: Output as predicted by SHAP attributions versus the actual output after dropping a particular feature.

We can see that while the prediction for *YearsEmployed* was roughly accurate, the predictions for *Age* and *Income* were both off by over three percentage points. Let us now extend the SHAP implementation to return error bounds and check if these prediction errors were within the confidence intervals. This is visualized in Figure 2.

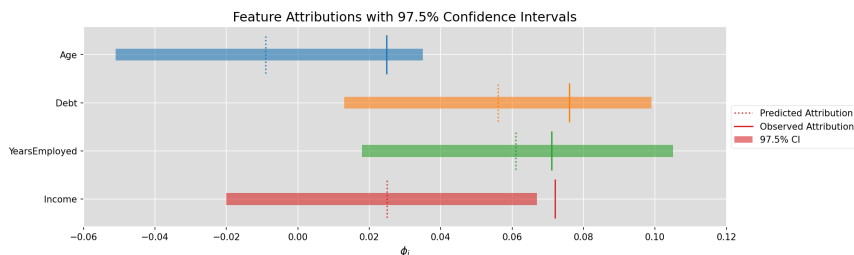


Figure 2: Computed 97.5% confidence intervals for each feature attribution, compared to the attributions returned by the original SHAP implementation (dotted) and the observed attributions (solid).

While three of our observed attributions are within the confidence interval, with *YearsEmployed* being most accurate as observed earlier, the

<sup>8</sup>This is another example of the background dataset selection problem; the null-output of 83.7% rejection produced by our background dataset is not nearly as intuitive or useful as a comparison against a 0% or 50% null-output.

**Income** attribution is outside the bounds. This could be due to a variety of factors, such as a large variance on  $f(x)$  or the predicted value reflecting large interaction effects when multiple features are dropped, but most likely is that our choice of  $B$  does not cover an adequate range of values of *Income*. In any case, extending the implementation to produce confidence intervals and evaluating these intervals against observed attributions is an excellent diagnostic tool for creating accurate explanatory models. For example, we can sample a number of  $x$  data points and look at the mean absolute error between predicted and observed attribution:

	Age	Debt	YearsEmployed	Income
MAE	0.083	0.061	0.071	0.055

Table 6: MAE of predicted attribution versus observed attributions for 100 samples of  $x$ , with  $B$  chosen as the first 100 training data points.

While this metric compares predicted attributions that take into account multiple feature interactions against observed attributions of single feature exclusion, it is a good rough indicator of the general accuracy of our explanatory model. Tools such as this MAE metric and observing how well various observed attributions align with predicted confidence intervals will be used to support the research described in Section 4.2, allowing background data selection techniques to be evaluated based on quantitative data.

## 5 Counterfactuals

### 5.1 Background

Counterfactual explanations, as proposed by Wachter et al. in 2017 [WMR17], are an increasingly important approach in providing transparency and explainability to the result of predictive models. In general terms, if we have a set of features  $x$  resulting in an outcome  $y = f(x)$ , where  $f(\cdot)$  is the model’s predictive function, a counterfactual explanation will provide us with an alternative set of input features  $x'$ , as close as possible to  $x$ , which results in a desired outcome  $y' = f(x')$ . The counterfactual method is well-suited for black-box model scenarios as it only requires access to the predictive function  $f(\cdot)$ .

A vast body of literature [VDH20] focuses on the desirable properties of counterfactuals and research specific conditions that might apply to counterfactual searches for different domains. In this paper, we will focus on three properties we consider fundamental in defining a counterfactual. These properties are *validity*, *sparsity* and *actionability*.

*Validity*, as defined in Wachter et al. [WMR17] defines formally the core aim of the counterfactual, which is to provide a set of features  $x'$ , as close as

possible to  $x$  and resulting in a desired outcome  $y'$ . That is, we are trying to minimize a distance between features,  $d(x, x')$ , for a predefined metric  $d$  and  $f(x') - y'$  for the outcomes, formally, we try to minimize the loss function

$$\mathbb{L}(x, x', y', \lambda) = \arg \min_{x'} \max_{\lambda} \lambda (f(x') - y')^2 + d(x, x'). \quad (14)$$

Typical choices for the distance metric  $d$  are, for instance, the  $L_1$  metric, defined as

$$d(x, x') = \sum_{i=1}^N |x_i - x'_i|. \quad (15)$$

*Actionability* refers to the ability to separate between *mutable* and *immutable* features in our input  $x$ . Due to legal requirements and fairness reasons, we might want to explore the feature space only regarding a specific subset of attributes  $\mathcal{A}$ . We can formally express validity, in terms of (14) as

$$\mathbb{L}(x, x', y', \lambda) = \arg \min_{x' \in \mathcal{A}} \max_{\lambda} \lambda (f(x') - y')^2 + d(x, x'). \quad (16)$$

Finally, we consider *sparsity* which is the desirable property that a counterfactual should change the least amount of features as possible. As stated in [VDH20] and [Mil19] this can have advantages regarding the model explainability itself, as it is simpler to conceptually visualize the alternative input for a smaller number of changed inputs. Formally, we can define *sparsity*, by adding a sparsity penalty term  $g(\cdot)$ , increasing with the number of features changed, to (16), resulting in

$$\mathbb{L}(x, x', y', \lambda) = \arg \min_{x' \in \mathcal{A}} \max_{\lambda} \lambda (f(x') - y')^2 + d(x, x') + g(x - x'). \quad (17)$$

Where, as in (14), a common choice of distance metric for  $g(\cdot)$  is the  $L_1$  metric as in (15). As stated in [VDH20, KS20] a possible heuristic for an acceptable number of changed features which doesn't endanger interpretability is two, at most.

Several methods are proposed in the literature to minimize the loss function  $\mathbb{L}$  in order to produce a counterfactual. For the case of a black-box model, a standard solution is to employ gradient-free numerical optimizations such as the Nelder-Mead [GCV<sup>+</sup>18] or Growing Sphere methods [LLM<sup>+</sup>18b] when the model is not differentiable, and gradient methods if dealing with differentiable models [KBBV20]. It is noteworthy that for these

methods, and for the common distance metrics applied, there is the issue of potential differences between the magnitude of the individual features. This is typically addressed by normalising the features in a pre-processing step or scaling the difference during the minimization step by some measure such as the feature-wise median absolute deviation [WMR17]. Since in this paper we are dealing with scenarios where we assume we do not have access to training data, we will omit this step.

The TrustyAI counterfactual implementation is based on stochastic sampling and heuristic search methods, namely using a Constraint Problem Solver (CPS). In the next section, we will describe how the search is performed using a CPS and its advantages.

## 5.2 Constraint problem solvers

In general terms, CPS are a family of algorithms that provide solutions by exploring a formally defined problem space (using constraints) to maximize a calculated score. For the counterfactual implementation we will use OptaPlanner [Sme06] as the CPS engine. In OptaPlanner constraints are divided mainly into *hard* and *soft*. Hard constraints represent states that cannot be accepted as a solution, while soft constraints represent a penalization of an acceptable solution.

A solution score  $\mathcal{S}$ , can consist of several components,  $\mathcal{S} = \{\mathcal{S}_1, \dots, \mathcal{S}_N\}$ , with each component representing a problem constraint. To implement a general counterfactual search as a constraint problem, the counterfactual properties presented in (14), (16) and (17) were mapped to constraints, along with some additional ones which we will look at. Denoting  $H_i$  as a hard constraint and  $S_i$  as a soft constraint, and assuming an input with  $N$  attributes, we can define our score  $\mathcal{S}$  as

$$\mathcal{S} = \{H_1, H_2, H_3, S_1, S_2\} \quad (18)$$

$$H_1 = - (f(x') - y')^2 \quad (19)$$

$$H_2 = - \sum_{a \in \mathcal{A}} \mathbf{1}(x_a \neq x'_a) \quad (20)$$

$$H_3 = - \sum_{i=1}^N \mathbf{1}(p_i(x'_i) < P_i) \quad (21)$$

$$S_1 = \sum_{i=1}^N d^*(x_i, x'_i) \quad (22)$$

$$d^*(x_i, x'_i) = \begin{cases} d(x_i, x'_i), & \text{if } x_i, x'_i \in \mathbb{N} \vee x_i, x'_i \in \mathbb{R} \\ 1 - \delta_{x, x'}, & \text{if } x_i, x'_i \text{ categorical} \end{cases} \quad (23)$$

$$S_2 = - \sum_{i=1}^N \mathbf{1}(x_i \neq x'_i) \quad (24)$$

We can see that (19) maps directly to the Euclidean distance between the counterfactual outcome and the original outcome, penalizing the solution the farther away it is, representing the *validity* property. The *actionability* property is represented by (20), where we penalize according to the total number of immutable attributes that were changed in the proposed counterfactual. A *confidence threshold* is represented by (21), which penalizes, attribute-wise, predictions with a probability below a provided threshold. If the model does not support prediction probabilities, this can be bypassed, whereas if they are supported, but it's not of interest for our counterfactual search, a default value of  $P = \{1, \dots, 1\}$  can be set, avoiding penalizing any solution on account of prediction probabilities. The input feature distance is represented as (22) and, as mentioned, a common metric is  $L_1$  as defined in (15), if the feature is numeric (continuous or discrete). If the feature is categorical, we calculate the distance as the feature-wise sum of indicators of whether the values have changed between  $x$  and  $x'$ . Finally, (24) represents the *sparsity* property, where we penalize the solution according to the total number of features changed. Although the score calculation, as implemented in TrustyAI, allows for using the training data, if available, in order to scale the distance using the mean absolute deviation, since we are considering the case where the training dataset is not available, we presented the score calculation as it is performed in this scenario.

OptaPlanner requires us to provide valid boundaries for the feature space in order to perform a search. These boundaries determine a region of interest for the counterfactual domain and do not prevent the application in the situation where training data is not available. The boundaries can be chosen using domain-specific knowledge, model meta-data or even from training



data, if available. For numerical, continuous or discrete, attributes we will specify an upper and lower bound,  $x_i \in [x_{i,lower}, x_{i,upper}[$  whereas for categorical attributes, we provide a set with all values to be evaluated during the search.

The actual counterfactual search is performed during OptaPlanner’s *Solver Phase*, consisting typically of a construction heuristic and a local search. The construction heuristic is responsible for instantiating counterfactual candidates using, for instance, a *First Fit* heuristic where counterfactual candidates are created, scored and the highest scoring selected. In the local search, which takes place after the construction heuristic, different methods can be applied such as *Hill Climbing* [SG06] or *Tabu* search [GL98]. *Tabu* search, for instance, selects the best scoring proposals and evaluates points in its vicinity until finding a higher scoring proposal, while maintaining a list of recent moves that should be avoided. The new candidates are then taken as the basis for the next round of moves, and the process is repeated until a termination criteria is met. *Tabu* search was the chosen method for the next section, however, one of the advantages of using OptaPlanner as the counterfactual search engine is that by defining the counterfactual search as a general constraints problem, different meta-heuristics can be swapped without having to reformulate the problem.

## 5.3 Experiments

### 5.3.1 Predictive model and data

The model used consisted of a random forest classifier trained with *scikit-learn* [PVG<sup>+</sup>11]. The model’s training data consisted of  $N_{obs} = 434$  observations of all numerical features, with the target being a credit card approval label of either 1 or 0, respectively *approved* or *not approved*<sup>9</sup>. The dataset contained 311 *not approved* applications, with the remaining labelled as *approved*. The inputs were **Age** (the applicant’s age in years), **Debt** (a debt score), number of years employed (**YearsEmployed**) and an **Income** value in thousands of USD. Detailed summary statistics are available in Table 7. We will refer to data points as  $x = \{Age, Debt, YearsEmployed, Income\}$  and outcomes/counterfactuals as  $y = y' = \{Approved\}$ .

### 5.3.2 Results

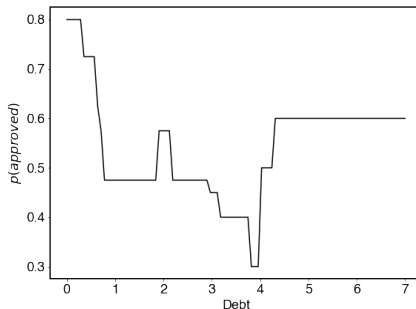
The first counterfactual search consisted of a repeated run of both the TrustyAI and Alibi<sup>10</sup> implementations to determine the counterfactual for a single input  $x$ . For both the implementations, a feature range was set as

<sup>9</sup>Kaggle Kerneler credit card approval dataset, <https://www.kaggle.com/kerneler/starter-credit-card-approval-b133d223-a>, last accessed 30/03/2021

<sup>10</sup>Alibi, <https://github.com/SeldonIO/alibi>, last accessed 29/03/2021.

Feature ( $x$ )	$\bar{x}(sd)$	Quartile					Search range	
		0%	25%	50%	75%	100%	$min$	$max$
Age	30.89 (11.99)	15.17	22.10	27.83	36.64	80.25	18.0	80.0
Debt	4.19 (4.55)	0.00	0.87	2.50	5.65	26.33	0.0	7.0
YearsEmployed	1.77 (2.82)	0.00	0.12	0.58	2.25	20.00	0.0	30.0
Income	35.18 (78.23)	0.00	0.00	0.00	17.75	367.00	0.0	300.0

Table 7: Summary statistics for the predictive model’s features.



(a)  $p(\text{Approved}|\text{Debt})$

Figure 3: Marginal of approved probability for *Debt* with a fixed set of features  $x_0$

detailed in Table 7. As mentioned previously, the distance metric used between the original data point,  $x$ , and a counterfactual  $x'$  was the  $L_1$  distance as defined in (15).

This initial search was performed, setting all the attributes as unconstrained, leaving the counterfactual implementation free to explore the entirety of the feature space. The Alibi counterfactual explainer was instantiated with an initial learning rate  $\eta_0 = 1$ , a target class of  $y' = 1$  with an associated target probability  $p(y') = 0.75$  with tolerance  $\epsilon = 0.24$ . The target probability is chosen in order to not be restrictive and cover  $0.51 \leq p(y') \leq 0.99$ .

The initial data point chosen was  $x_0 = \{21.0, 3.5, 5.0, 100.0\}$  which the model classified as  $y_0 = \{0\}$  with  $p(y_0) = 0.6$ .

Results for this counterfactual search, including mean computational time, sparsity score and  $L_1$  distance are in Table 8.

We can see that both implementations achieve similar results, namely  $y' = \{1\}$  with  $p(y'_{Alibi}) = 0.6$ ,  $p(y'_{TrustyAI}) = 0.55$  with comparable distances  $L_1(x, x')$ , but with some important differences. Alibi’s counterfactual had a lower sparsity score, changing three attributes in contrast to TrustyAI, which changed one, and the mean computational time was much lower in TrustyAI than Alibi. TrustyAI returns a valid counterfactual after a few iterations, and this can be visualized on Figure 8, where we can see that when running

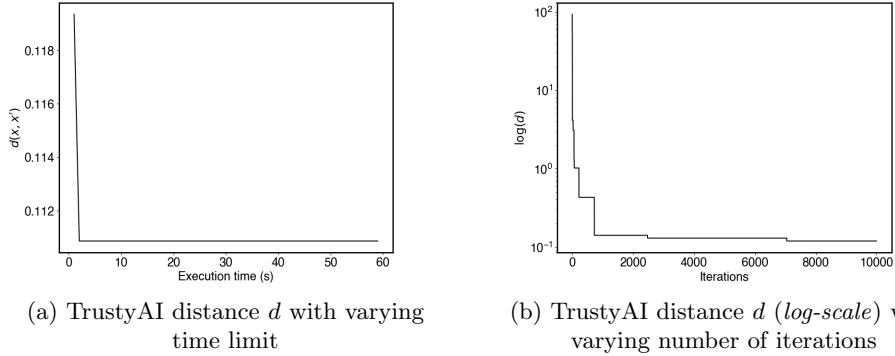


Figure 4: TrustyAI distance  $d$  for counterfactual searches with varying time limit and number of iterations.

Implementation	$N_{runs}$	$y'$	Sparsity	$\bar{d}$	Mean time (s)
Alibi	10	{20.8679, 4.0230, 5.0157, 100.0}	-3	0.5557	52.10
TrustyAI	100	{21.0, 4.0221, 5.0, 100.0}	-1	0.52210	1.93

Table 8: Computational time and counterfactual  $L_1$  distance for the fully unconstrained counterfactual search using Alibi and TrustyAI. Mean computational time and  $L_1$  distance between original features and counterfactual for  $N = 10$  runs. Sparsity indicates the number of features changed compared to the original.  $y'$  is a counterfactual search result randomly selected from one of the runs.

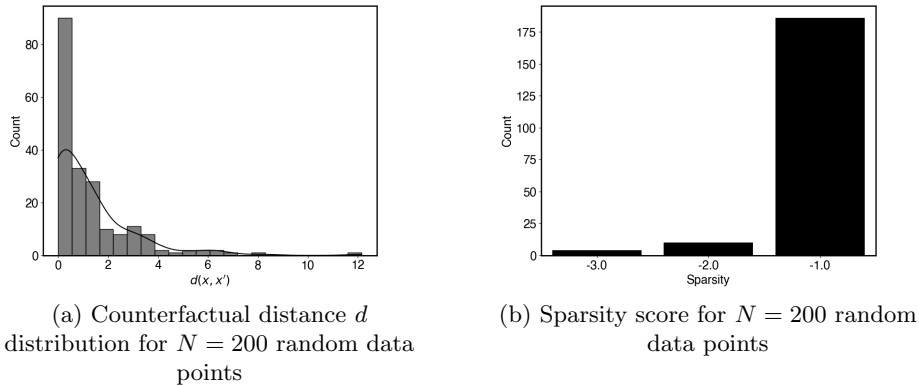


Figure 5: Distance  $d$  and sparsity score for  $N = 200$  runs of a counterfactual search for randomly generated inputs  $x$ .

the search for a varying number of iteration steps, the distance  $d$  stabilizes on its final value after approximately 1000 iterations or approximately 2 seconds. Since the feature with the largest change in both implementations is the *debt score*, we can plot (Figure 3) the marginal probability of  $p(y = \{1\})$  for fixed inputs *Age*, *YearsEmployed* and *Income* as in  $x_0$ . Intuitively we can see that both implementations correctly select the closest **Debt** outcome change point around  $debt \approx 4.0$ , rather than (the higher probability, but also farther away)  $debt \approx 0.7$ .

A stability benchmark was also produced to measure the TrustyAI counterfactual behaviour for repeated searches with different randomly select inputs. Data points were randomly generated from a uniform distribution within the boundaries of one of the  $N$  features in Table 7, that is

$$x_i \sim \mathcal{U}(x_{i,min}, x_{i,max}), \quad i = 1, \dots, N \quad (25)$$

and from this set,  $N_{obs} = 200$  inputs were randomly sampled from the ones that produced an outcome  $y = \{0\}$ . This resulted in a dataset that covered a wide range of features values combinatorially. A counterfactual search for the desired outcome  $y' = \{1\}$  was then performed for each data point. The search result would provide us with whether a counterfactual was found and, if so, the associated distance  $d(\cdot)$  and the sparsity score. The results are presented in Figure 5.

From this dataset, the search was able to find a valid counterfactual ( $y' = \{1\}$ ) for 197 data points out of 200. From those with valid counterfactuals, we can see in Figure 5 that the feature distance is very likely to be close to zero and decrease frequency with magnitude, a behaviour we were expecting to see. Figure 5 also shows that the overwhelming majority

of the valid counterfactual changed a single feature, which was one of our desired properties and satisfying the guidance in [KS20] of a maximum of two features changed.

## 6 Conclusions

In this paper we have presented the TrustyAI Explainability Toolkit, a XAI toolkit that can work seamlessly on AI based systems as well as decision services. We introduced three explainability algorithms covering generation of saliency and counterfactual explanations.

Local explanations generated with *TrustyAI-LIME* are more effective than LIME reference implementation (up to 0.52 higher impact-score when compared to *LIME-cont*) on our benchmark. Additionally, our solution does not require training data to accurately sample and encode perturbed samples, which make it fit better in the decision service scenario. We plan to deepen our understanding of the effect of our approach by also studying consequences on the stability of the generated explanations.

The planned extensions to SHAP within TrustyAI-SHAP have the potential to greatly improve diagnostic ability when designing explainers. In the existing implementation of SHAP, there are no heuristics by which to choose background data, which can lead to unhelpful and unintuitive feature attributions. Meanwhile, feature attributions that are presented without confidence intervals have been demonstrated to lead to inaccurate ranking of feature importance. TrustyAI-SHAP aims to address these issues through research into background data choice heuristics and techniques, as by providing accuracy metrics and confidence intervals to accompany feature attributions.

One of the advantages of using an open-source, modular engine for CSP, such as OptaPlanner, is the ability to abstract the score calculation and problem formulation (in terms of inputs, outputs and constraints) from the actual search algorithm. This brings the freedom to use different search meta-heuristics for different scenarios and choose between the most suited for the problem at hand. The formulation of the inputs, output and goals can also be extended to include other types of data, as long as a distance function between the new feature types can be defined. Overall, for the model used in this paper, the TrustyAI counterfactual search achieved good performance relative to the Alibi baseline. When performing repeated searches for a single input, both implementations had a high degree of consistency, both in terms of the counterfactual proximity, sparsity score, and computational time. TrustyAI requires significantly less time to retrieve a valid counterfactual. However, care must be taken when interpreting this result since there are several factors to be addressed in future work, such as benchmarking for more complex models and non-numerical features. Additionally, Tensorflow

can carry considerable overhead for shorter runs, so it is possible that the computational time difference can narrow in other scenarios. In terms of sparsity, TrustyAI manages to fully satisfy the requirement of changing the least amount of features as possible. Since sparsity is explicitly coded as a component of the score penalization this affords more significant guarantees regarding the final result. Regarding the validity, we observed that the counterfactual behaved as expected when analyzing the changed feature’s predictive outcome marginal. A stability test was also performed, randomly sampling inputs, resulting in a non-approved outcome, from the feature space. The search for counterfactuals was successful for the overwhelming majority of inputs (99.85%), with the vast majority of counterfactuals having a calculated distance close to zero, with an expected distance distribution. Regarding the sparsity score, the stability test also showed that counterfactual search favours the lowest possible score (one changed feature), providing greater interpretability of the counterfactual explanation and keeping in line with the literature’s guidelines. Overall, we consider that a CSP-based counterfactual search implementation constitutes a viable alternative to the already existing methods, both in terms of practical results for a real-world scenario and as a research framework due to the ease of experimentation with different search algorithms and feature types.

## References

- [ABC<sup>+</sup>16] Martin Abadi, Paul Barham, Jianmin Chen, Zhifeng Chen, Andy Davis, Jeffrey Dean, Matthieu Devin, Sanjay Ghemawat, Geoffrey Irving, Michael Isard, Manjunath Kudlur, Josh Levenberg, Rajat Monga, Sherry Moore, Derek G. Murray, Benoit Steiner, Paul Tucker, Vijay Vasudevan, Pete Warden, Martin Wicke, Yuan Yu, and Xiaoqiang Zheng. Tensorflow: A system for large-scale machine learning. In *12th USENIX Symposium on Operating Systems Design and Implementation (OSDI 16)*, pages 265–283, 2016.
- [ADRDS<sup>+</sup>20] Alejandro Barredo Arrieta, Natalia Díaz-Rodríguez, Javier Del Ser, Adrien Bennetot, Siham Tabik, Alberto Barbado, Salvador García, Sergio Gil-López, Daniel Molina, Richard Benjamins, et al. Explainable artificial intelligence (xai): Concepts, taxonomies, opportunities and challenges toward responsible ai. *Information Fusion*, 58:82–115, 2020.
- [AKF20] Sule Anjomshoae, Timotheus Kampik, and Kary Främling. Py-ciu: A python library for explaining machine learning predictions using contextual importance and utility. In *IJCAI-*

*PRICAI 2020 Workshop on Explainable Artificial Intelligence (XAI)*, 2020.

- [Ath17] Susan Athey. Beyond prediction: Using big data for policy problems. *Science*, 355(6324):483–485, 2017.
- [BHLL20] Steven Bramhall, Hayley Horn, Michael Tieu, and Nibhrat Lohia. Qlime-a quadratic local interpretable model-agnostic explanation approach. *SMU Data Science Review*, 3(1):4, 2020.
- [Bie18] Przemysław Biecek. Dalex: explainers for complex predictive models in r. *The Journal of Machine Learning Research*, 19(1):3245–3249, 2018.
- [ESB19] D. Etinger, S. D. Simić, and L. Buljubašić. Automated decision-making with dmn: from decision trees to decision tables. In *2019 42nd International Convention on Information and Communication Technology, Electronics and Microelectronics (MIPRO)*, pages 1309–1313, 2019.
- [GCV<sup>+</sup>18] Rory Mc Grath, Luca Costabello, Chan Le Van, Paul Sweeney, Farbod Kamiab, Zhao Shen, and Freddy Lecue. Interpretable credit application predictions with counterfactual explanations. *arXiv preprint arXiv:1811.05245*, 2018.
- [GL98] Fred Glover and Manuel Laguna. Tabu search. In *Handbook of combinatorial optimization*, pages 2093–2229. Springer, 1998.
- [Glo89] Fred Glover. Tabu search—part i. *ORSA Journal on computing*, 1(3):190–206, 1989.
- [Gun17] David Gunning. Explainable artificial intelligence (xai). *Defense Advanced Research Projects Agency (DARPA)*, *nd Web*, 2(2), 2017.
- [HDVS20] F. Hasić, J. De Smedt, S. Vanden Broucke, and E. Serral Asensio. Decision as a service (daas): A service-oriented architecture approach for decisions in processes. *IEEE Transactions on Services Computing*, pages 1–1, 2020.
- [KBBV20] Amir-Hossein Karimi, Gilles Barthe, Borja Balle, and Isabel Valera. Model-agnostic counterfactual explanations for consequential decisions. In *International Conference on Artificial Intelligence and Statistics*, pages 895–905. PMLR, 2020.
- [KS20] Mark T Keane and Barry Smyth. Good counterfactuals and where to find them: A case-based technique for generating

- counterfactuals for explainable ai (xai). In *International Conference on Case-Based Reasoning*, pages 163–178. Springer, 2020.
- [KVLVC19] Janis Klaise, Arnaud Van Looveren, Giovanni Vacanti, and Alexandru Coca. Alibi: Algorithms for monitoring and explaining machine learning models, 2019.
- [LBS<sup>+</sup>19] Eunjin Lee, David Braines, Mitchell Stiffler, Adam Hudler, and Daniel Harborne. Developing the sensitivity of lime for better machine learning explanation. In *Artificial Intelligence and Machine Learning for Multi-Domain Operations Applications*, volume 11006, page 1100610. International Society for Optics and Photonics, 2019.
- [LL17] Scott Lundberg and Su-In Lee. A unified approach to interpreting model predictions. *Advances in Neural Information Processing Systems*, 2017.
- [LL21] Scott Lundberg and Su-In Lee. <https://github.com/slundberg/shap>, 2021. ”Accessed Mar. 30, 2021”.
- [LLM<sup>+</sup>18a] Thibault Laugel, Marie-Jeanne Lesot, Christophe Marsala, Xavier Renard, and Marcin Detyniecki. Comparison-based inverse classification for interpretability in machine learning. In Jesús Medina, Manuel Ojeda-Aciego, José Luis Verdegay, David A. Pelta, Inma P. Cabrera, Bernadette Bouchon-Meunier, and Ronald R. Yager, editors, *Information Processing and Management of Uncertainty in Knowledge-Based Systems. Theory and Foundations*, pages 100–111, Cham, 2018. Springer International Publishing.
- [LLM<sup>+</sup>18b] Thibault Laugel, Marie-Jeanne Lesot, Christophe Marsala, Xavier Renard, and Marcin Detyniecki. Comparison-based inverse classification for interpretability in machine learning. In *International Conference on Information Processing and Management of Uncertainty in Knowledge-Based Systems*, pages 100–111. Springer, 2018.
- [LLS<sup>+</sup>17] Michael T Lash, Qihang Lin, Nick Street, Jennifer G Robinson, and Jeffrey Ohlmann. Generalized inverse classification. In *Proceedings of the 2017 SIAM International Conference on Data Mining*, pages 162–170. SIAM, 2017.



- [LRL<sup>+</sup>18] Thibault Laugel, Xavier Renard, Marie-Jeanne Lesot, Christophe Marsala, and Marcin Detyniecki. Defining locality for surrogates in post-hoc interpretability. *arXiv preprint arXiv:1806.07498*, 2018.
- [LSB<sup>+</sup>19] Z. Lin, M. Shafiee, S. Bochkarev, Michael St. Jules, X. Y. Wang, and A. Wong. Do explanations reflect decisions? a machine-centric strategy to quantify the performance of explainability algorithms. *ArXiv*, abs/1910.07387, 2019.
- [Mil19] Tim Miller. Explanation in artificial intelligence: Insights from the social sciences. *Artificial intelligence*, 267:1–38, 2019.
- [NJKC19] Harsha Nori, Samuel Jenkins, Paul Koch, and Rich Caruana. Interpretml: A unified framework for machine learning interpretability. *arXiv preprint arXiv:1909.09223*, 2019.
- [PVG<sup>+</sup>11] Fabian Pedregosa, Gaël Varoquaux, Alexandre Gramfort, Vincent Michel, Bertrand Thirion, Olivier Grisel, Mathieu Blondel, Peter Prettenhofer, Ron Weiss, Vincent Dubourg, et al. Scikit-learn: Machine learning in python. *the Journal of machine Learning research*, 12:2825–2830, 2011.
- [RSG16] Marco Tulio Ribeiro, Sameer Singh, and Carlos Guestrin. ” why should i trust you?” explaining the predictions of any classifier. In *Proceedings of the 22nd ACM SIGKDD international conference on knowledge discovery and data mining*, pages 1135–1144, 2016.
- [SDF20] Sheng Shi, Yangzhou Du, and Wei Fan. An extension of lime with improvement of interpretability and fidelity. *arXiv preprint arXiv:2004.12277*, 2020.
- [SG06] Bart Selman and Carla P Gomes. Hill-climbing search. *Encyclopedia of cognitive science*, 81:82, 2006.
- [SGK17] Avanti Shrikumar, Peyton Greenside, and Anshul Kundaje. Learning important features through propagating activation differences. *CoRR*, abs/1704.02685, 2017.
- [Sha53] Lloyd Shapley. A value for n-person games. *Contributions to the Theory of Games*, 2.28, 1953.
- [Sme06] GD Smet. Optaplanner open source constraint solver, 2006.
- [SSrHF19] Kacper Sokol, R Santos-rodriguez, A Hepburn, and Peter Flach. Surrogate prediction explanations beyond lime. *no. HCML*, 2019.

- [TWB<sup>+</sup>20] Ian Tenney, James Wexler, Jasmijn Bastings, Tolga Bolukbasi, Andy Coenen, Sebastian Gehrmann, Ellen Jiang, Mahima Pushkarna, Carey Radebaugh, Emily Reif, and Ann Yuan. The language interpretability tool: Extensible, interactive visualizations and analysis for NLP models, 2020.
- [VBC20a] Giorgio Visani, Enrico Bagli, and Federico Chesani. Optilime: Optimized lime explanations for diagnostic computer algorithms. *arXiv preprint arXiv:2006.05714*, 2020.
- [VBC<sup>+</sup>20b] Giorgio Visani, Enrico Bagli, Federico Chesani, Alessandro Poluzzi, and Davide Capuzzo. Statistical stability indices for lime: obtaining reliable explanations for machine learning models. *arXiv preprint arXiv:2001.11757*, 2020.
- [VDH20] Sahil Verma, John Dickerson, and Keegan Hines. Counterfactual explanations for machine learning: A review. *arXiv preprint arXiv:2010.10596*, 2020.
- [VG19] Manisha Verma and Debasis Ganguly. Lirne: locally interpretable ranking model explanation. In *Proceedings of the 42nd International ACM SIGIR Conference on Research and Development in Information Retrieval*, pages 1281–1284, 2019.
- [VŠ21] Domen Vreš and Marko Robnik Šikonja. Better sampling in explanation methods can prevent dieselgate-like deception. *arXiv preprint arXiv:2101.11702*, 2021.
- [Wen21] K Wendel. Local explanations for hyperspectral image classification: Extending the local interpretable model-agnostic explanation approach with principal components. 2021.
- [WMR17] Sandra Wachter, Brent Mittelstadt, and Chris Russell. Counterfactual explanations without opening the black box: Automated decisions and the gdpr. *Harv. JL & Tech.*, 31:841, 2017.
- [WPB<sup>+</sup>19] James Wexler, Mahima Pushkarna, Tolga Bolukbasi, Martin Wattenberg, Fernanda Viégas, and Jimbo Wilson. The what-if tool: Interactive probing of machine learning models. *IEEE transactions on visualization and computer graphics*, 26(1):56–65, 2019.
- [ZSEv12] A. Zarghami, B. Sapkota, M. Z. Eslami, and M. van Sinderen. Decision as a service: Separating decision-making from application process logic. In *2012 IEEE 16th International*